cies, empirical observations suggest that ferric iron, predominantly hosted in garnet, behaves relatively incompatibly during melting, forming oxidized melts and reduced residues (*14*). In the spinel facies, ferric iron, principally accommodated in spinel, may behave more compatibly and be partly retained in the residue.

If heavy $\delta^{57/54}$Fe and $\Delta\log f_{O_2}$values are generally applicable to garnet-facies melting residues, then a finite difference may exist between the $\delta^{57/54}$Fe and $\Delta\log f_{O_2}$ values of magmas produced by partial melting of garnet and spinel-facies mantle. However, oceanic island basalts (OIB) have only slightly higher $\Delta\log f_{O_2}$ (~ 0.8 log-bar units) values than mid-ocean ridge basalts (MORB) (*19*, *20*), and fractionally different average $\delta^{57/54}$Fe values (MORB, 0.18‰; OIB, 0.12‰) (*21*). OIBs may become oxidized relative to their source during melt segregation and decompression (*9*). If so, their more oxidized nature and lighter $\delta^{57/54}$Fe values may indicate that magma $\delta^{57/54}$Fe and $\Delta\log f_{O_2}$ values are coupled and controlled by melting regime and source mineralogy and do not directly reflect the $\delta^{57/54}$Fe and $\Delta\log f_{O_2}$ values of their source region. This limited variation in the $\Delta\log f_{O_2}$ values of MORB and OIB, compared to peridotites, may explain why previous studies of iron isotopes in mafic rocks, dominantly MORB and OIB (*21*), did not reveal large iron isotope variations.

Our results are readily explained if variations in spinel and bulk-rock $\delta^{57/54}$Fe are caused by melt-extraction processes accompanied by changes in mantle $\Delta\log f_{O_2}$. Although the $Fe^{3+}/\Sigma Fe$ of whole rocks and spinels can become decoupled from $\Delta\log f_{O_2}$ (*2*), the absence of outliers on the trend of $\delta^{57/54}$Fe and $\Delta\log f_{O_2}$ (Fig. 1A) suggests that iron isotopes in spinels are more resistant to resetting than spinel $Fe^{3+}/\Sigma Fe$. This is consistent with the observation that spinels from the metasomatized Simcoe xenoliths are displaced above the trend of $\delta^{57/54}$Fe with spinel $Fe^{3+}/\Sigma Fe$ (Fig. 1B), yet lie on the correlation between $\delta^{57}Fe/^{54}Fe$ and $\Delta\log f_{O_2}$. Hence, iron isotopes provide an independent means of estimating $\Delta\log f_{O_2}$ that can complement existing methods.

References and Notes

1. D. Canil, *Earth Planet. Sci. Lett.* **195**, 75 (2002).
2. J. W. Delano, *Orig. Life Evol. Biosph.* **31**, 311 (2001).
3. X. K. Zhu *et al.*, *Earth Planet. Sci. Lett.* **200**, 47 (2002).
4. V. B. Polyakov, S. D. Mineev, *Geochim. Cosmochim. Acta* **64**, 849 (2000).
5. E. A. Schauble, G. R. Rossman, H. P. Taylor Jr., *Geochim. Cosmochim. Acta* **65**, 2487 (2001).
6. H. S. O'Neill, V. J. Wall, *J. Petrol.* **28**, 1169 (1987).
7. B. J. Wood, L. T. Dryndzie, K. L. Johnson, *Science* **248**, 337 (1990).
8. C. Ballhaus, R. F. Berry, D. H. Green, *Contrib. Mineral. Petrol.* **107**, 27 (1991).
9. C. Ballhaus, *Contrib. Mineral. Petrol.* **114**, 331 (1993).
10. J. F. Luhr, J. J. Aranda-Gómez, *J. Petrol.* **38**, 1075 (1997).
11. D.-C. Lee *et al.*, *J. Petrol.* **37**, 415 (1996).
12. A. D. Brandon, D. S. Draper, *Geochim. Cosmochim. Acta* **60**, 1739 (1996).
13. I. J. Parkinson, R. J. Arculus, *Chem. Geol.* **160**, 409 (1999).
14. A. B. Woodland, M. Koch, *Earth Planet. Sci. Lett.* **214**, 295 (2003).
15. V. S. Kamenetsky, A. J. Crawford, S. Meffre, *J. Petrol.* **42**, 655 (2001).
16. R. J. Arculus, *Lithos* **33**, 189 (1994).
17. P. B. Kelemen, *J. Petrol.* **31**, 51 (1990).
18. Materials and methods are available as supporting material on *Science* Online.
19. A. Kiline, I. S. E. Carmichael, M. L. Rivers, R. O. Sack, *Contrib. Mineral. Petrol.* **83**, 136 (1983).
20. D. M. Christie, I. S. E. Carmichael, C. H. Langmuir, *Earth Planet. Sci. Lett.* **79**, 397 (1986).
21. B. L. Beard *et al.*, *Chem. Geol.* **195**, 87 (2003).
22. P. R. Wells, *Contrib. Mineral. Petrol.* **62**, 129 (1977).
23. J.-C. C. Mercier, *Tectonophysics* **70**, 1 (1980).
24. P. Nimis, P. Ulmer, *Contrib. Mineral. Petrol.* **133**, 122 (1998).
25. G. P. Brey, T. Kohler, *J. Petrol.* **31**, 1353 (1990).

26. This paper benefited from discussions with J. Connolly, D. Harrison, T. Holland, R. Kessell, S. Nielsen, I. Parkinson, R. Powell, U. Wiechert, and P. Ulmer. O. Jagoutz provided invaluable help in collecting the Kohistan samples. We thank D. Barford, A. Brandon, D.-C. Lee, J. Luhr, and M. Rehkämper for providing additional samples. We also thank C. Stirling, F. Oberli, and U. Menet for technical help. This project was supported by ETH Zürich and the Swiss National Fonds (grant 20-61465.00 to J.-P. B.).

Supporting Online Material
www.sciencemag.org/cgi/content/full/304/5677/1656/DC1
Materials and Methods
Tables S1 and S2
References

15 January 2004; accepted 6 May 2004

New Zealand Maritime Glaciation: Millennial-Scale Southern Climate Change Since 3.9 Ma

Robert M. Carter* and Paul Gammon

Ocean Drilling Program Site 1119 is ideally located to intercept discharges of sediment from the mid-latitude glaciers of the New Zealand Southern Alps. The natural gamma ray signal from the site's sediment core contains a history of the South Island mountain ice cap since 3.9 million years ago (Ma). The younger record, to 0.37 Ma, resembles the climatic history of Antarctica as manifested by the Vostok ice core. Beyond, and back to the late Pliocene, the record may serve as a proxy for both mid-latitude and Antarctic polar plateau air temperature. The gamma ray signal, which is atmospheric, also resembles the ocean climate history represented by oxygen isotope time series.

Recent comparisons between climate proxies from subpolar sediment cores and polar ice cores suggest that Southern Hemisphere events lead those from the north by ~1.5 to 3 thousand years (ky) (*1–3*). In reality, two geographical data points located near opposing poles are inadequate to allow such a unique causality and time lag to be inferred (*4*). A better understanding of climate dynamics with respect to the coupling of the Northern and Southern Hemispheres therefore requires the assembly of additional climate records across the critical mid-latitude temperate zones. Here we present a 3.9 million year (My)–long record of glaciation in the New Zealand Southern Alps, as preserved in a core through intermediate water-depth sediment drifts from Ocean Drilling Program (ODP) Site 1119, east of South Island, in the southwest Pacific Ocean (Fig. 1).

The New Zealand Southern Alps are a 600-km-long chain of mountains that today host more than 3000 glaciers individually larger than 0.01 km^2, with a total area of 1159 km^2 and a combined ice volume of 53 km^3 (*5*). Temperate maritime glaciers are particularly sensitive to climate perturbations because of their high accumulation and ablation rates (*6*). The mid-latitude location of the Southern Alps, at the junction between subtropical and polar air masses and near major ocean fronts such as the Subtropical Front (STF), adds even more to their sensitivity as a monitor of climatic change.

It is currently controversial whether recent climate fluctuations from mid-latitude New Zealand relate primarily to Northern or Southern Hemisphere polar records (*7–10*). The Site 1119 record, when compared at millennial resolution with that of the Vostok ice core, shows that New Zealand climate cyclicity resembles that of Antarctica back to at least Marine Isotope Stage (MIS) 11, ~0.37 million years ago (Ma) (*11*). This level corresponds to the present base of the Antarctic ice core record. Beyond it, the cyclicity in the 1119 core records a changing mid-latitude ice signal that may continue to serve as a proxy for Antarctic polar plateau air

School of Earth and Environmental Sciences, University of Adelaide, Adelaide, SA 5005, Australia.

*To whom correspondence should be addressed. E-mail: bob.carter@jcu.edu.au

temperature even as far back as ~3.9 Ma [MIS Gisla (Gi)11] in the Late Pliocene. The climatic proxy represented by natural gamma ray measurements from Site 1119 exhibits many close similarities with but also some important differences from the standard climatic histories that are inferred from the deep-sea oxygen isotope record (*12*).

A complete natural gamma ray emission record was assembled for ODP Site 1119 (*13*) using both onboard multisensor track (MST) and downhole geophysical log measurements (*14*). We interpret the Site 1119 gamma ray signal as representing fluctuations in clay content that correspond to variations in the rate of supply of glacial "rock flour" from a waxing and waning South Island ice cap. The cyclic climate signal has a resolution of 0.1 to 0.6 ky back to MIS 17 (0.69 Ma) and 1 to 2.2 ky for the older portions of the hole back to 3.9 Ma.

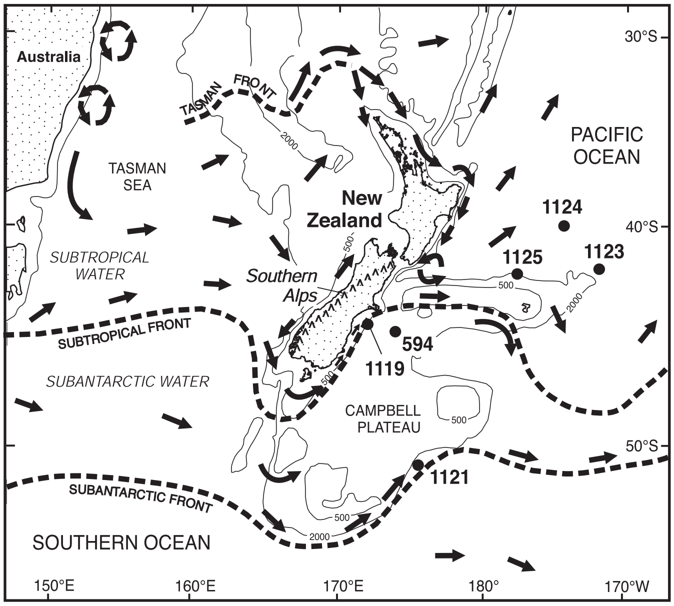

Fig. 1. Locality map of ODP sites, showing also the major bathymetric and oceanographic features of the southwest Pacific region.

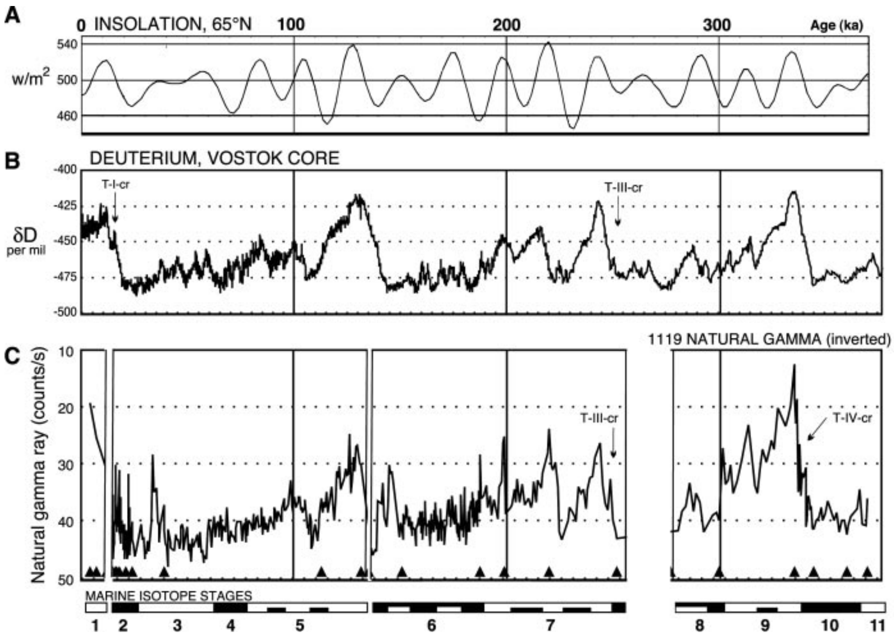

Fig. 2. Comparison between climate signals from ODP Site 1119 and Vostok, Antarctica, over the last 0.37 My. (**A**) Insolation curve for latitude 65°N. (**B**) Deuterium isotope ratio (δD) for the Vostok ice core (*15*). (**C**) Natural gamma ray signal from ODP Site 1119 (the scale is reversed) (*13*). Black triangles indicate age tie points between Site 1119 and Vostok; diamond bullets, the location of warm gamma anomalies in MIS 2 to 3 and 6 (the latter anomaly also occurs in the oxygen isotope record at DSDP Site 594) (*17*, *18*). These features are site-specific and result from seaward movement of the STF and its probable merging with the SAF into an intense combined frontal zone, driven by the lowered sea level at glacial maxima (*11*). Termination I, III, and IV cold reversals are labeled T-I-cr, T-III-cr, and T-IV-cr, respectively.

A comparison between the Site 1119 natural gamma ray record and the Vostok deuterium isotope record (which is a proxy for air temperature above the Antarctic polar plateau) (*15*) back to 0.37 Ma (MIS 11) is shown in Fig. 2. A high sedimentation rate and rapidly shallowing water occurred at Site 1119 during the MIS 15 glacial cycle. As a result, the background climatic signal of that time is overprinted in the sedimentary record by site-specific shallow-water oceanographic features, including especially those that result from climate and sea-level forced movements of the STF (*11*). Despite this, the 1119 gamma record exhibits a clear climatic signal at Milankovitch periodicities throughout MIS 1 to 11.

The climatic patterning of some Antarctic ice cores across the MIS 1 to 5 interval resembles that of cores from Greenland (*3*). In contrast, this interval at Site 1119 matches the Vostok record (*15*) much more closely than it does that of Greenland (*16*). And for the MIS 7 and MIS 8 to 11 periods, for which the equivalent sediments at Site 1119 were deposited in deeper, less disturbed waters, the match between the New Zealand and Antarctic climatic records is markedly close at both the 1- to 2-ky and the Milankovitch 20- and 41-ky scales of resolution. Finally, small features such as the Termination III and Termination IV (multiple) cold reversals appear in amplified form in the New Zealand record (Fig. 2), perhaps indicating an enhanced climatic sensitivity resulting from the maritime location.

Large "warm" gamma ray and oxygen isotope anomalies occur at Site 1119 within cold periods MIS 2 to 3 and 6. Similar warm anomalies have been recorded in the oxygen isotope records of nearby Deep-Sea Drilling Program (DSDP) Site 594 (*17*) and International Marine Past Global Changes Studies (IMAGES) core MD97-2102 (*18*). These features do not represent climatic warming per se, but rather reflect local changes in water mass (perhaps including jetting through the Mernoo Gap) and frontal disposition during climate cycling (*11*). Forced by the interaction of a falling sea level and bathymetry, the STF off eastern South Island moved southeastward during climatic deteriorations. At the same time, in the open ocean the Subantarctic Front (SAF) moved north, causing accentuation of Antarctic Circumpolar Current (ACC) flow along the eastern Campbell Plateau–Bounty Trough gyre path, which bounds the ACC to the northwest and is itself also bathymetrically controlled. During peak glaciations, these two effects combined to cause the STF and SAF to coalesce into a zone of intense oceanographic gradients offshore from eastern South Island (*19*). Thus, rather than indicating that "extrapolar climates in the Southern Hemisphere were more variable than is inferred on the basis of Antarctic ice cores alone" (*20*) and that climatic decoupling occurred between the mid-latitudes and Antarctica during glaciations, the warm anomalies at Sites 594, 1119, and MD97-2120 represent site-specific, local phenomena. Meanwhile, the similarity of the atmospheric records at Site 1119 and Vostok throughout MIS 7 to 11 indicates of itself that close climatic coupling persisted across southern latitudes during both glacial and interglacial periods.

The lower resolution that is apparent in the 1119 record during MIS 5.5, 7, and 9 (Fig. 2) is caused by reduced sedimentation rates (and, generally, the presence of sand) and precludes a detailed comparison of those parts of the record with that of Vostok. For MIS 2 to 4, parts of which show a millennial or higher resolution at Site 1119, site-specific oceanographic features obscure the match between the two records. However, the two climatic histories can be compared at millennial scale over a 40-ky-long interval within MIS 6, between 150 and 190 ky ago. This comparison (supporting text) shows a prima facie correspondence between the millennial climate cyclicity manifest in the Site 1119 gamma record, the Vostok deuterium isotope record, and a high-resolution oxygen isotope record from nearby MD97-2120 (*20*) (Fig. 3). The lack of detailed independent dating means that the apparent match of these three MIS 6 records must be treated with caution. But even the most conservative interpretation of the data suggests the existence of a close and perhaps even submillennial link between New Zealand and Antarctic climate, and therefore the presence of strong atmospheric coupling across a wide span of Southern Hemisphere latitudes. In essence, New Zealand climate dances to the hymn of Antarctica, not Greenland.

Two features are immediately apparent in the complete composite gamma ray log for Site 1119 down to the base of hole C (Fig. 4C). First, a dominant ~40-ky cyclicity occurs throughout the core and is of similar magnitude and symmetry to equivalent high-resolution oxygen isotope curves (Fig. 4, E to G). Second, climatic events are represented with an average resolution of 1.3 ky, or even higher (0.5 ky) over the high-sedimentation part of the core younger than ~0.68 Ma (Fig. 4D). Close inspection of the gamma ray record suggests that it may encompass peaks and troughs equivalent to all, or nearly all, of the marine isotope stages back to Gi11 at 3.9 Ma. Only occasionally does the manifestation of a climate cycle in the Site 1119 gamma ray record differ markedly from its oxygen isotope equivalent, for example, the broad and subdued nature of the peak representing MIS 21. Where the record passes from one (seismically delimited) sediment drift to another, parts of an individual stage may perhaps have been truncated. However, sediment drift deposition generally appears to have been so steady that oxygen isotope stages may continue uninterrupted even across drift boundaries.

The gamma ray record of Site 1119 reflects the balance between freeze and thaw in the alpine ice cap of the New Zealand Southern Alps. Therefore, to the New Zealand–Antarctica atmospheric and oceanic climatic coupling that we demonstrated earlier can now be added a New Zealand–Antarctica–global ocean coupling that registers equivalent climatic events down to millennial scale. These events—for time scales beyond those of polar ice cores—have hitherto been represented primarily by oxygen isotope curves alone. Subtle longer term climatic trends exhibited by Pacific isotope curves (several to many hundred thousand years long) are present also in the gamma ray record at Site 1119, generally with amplification. These features include (i) a long-term cooling trend since ~3 Ma, as marked also by steady long-term enrichment of the Site 1119 oxygen isotope signature (Fig. 4); (ii) long wavelength modulation of the gamma record in sympathy with the movements of the STF that are reflected in the carbon isotope record (*11*, *14*); and (iii) the presence of particularly severe cooling intervals at 3.63 to 3.68 Ma (MIS Gi2 to Gi4), 3.38 Ma (MIS 146), 3.12 Ma (MIS 132), 2.72 Ma (MIS 108), 2.53 Ma (MIS 100), 1.79 Ma (MIS 66), 1.53 Ma (MIS 52), and 0.43 Ma (MIS 12); and (iv) the occurrence of unusually warm interglacial episodes at 3.52 Ma (MIS 151), 3.16 Ma (MIS 135), 2.99 Ma (MIS 121), 2.39 Ma (MIS 93), 1.60 Ma (MIS 55), 1.24 Ma (MIS 37), 0.95 Ma (MIS 25), and 0.33 Ma (MIS 9) (Fig. 4).

In conclusion, a clear relationship has existed between millennial climate variations on the Antarctic ice cap, in the glaciers of the mid-latitude New Zealand Southern Alps, and in the oceanic oxygen isotope record, for at least the past 0.37 My. Though we cannot yet demonstrate an exact synchrony between the mid-latitude and polar regions for individual climatic events, such equivalence would be consistent with the data presented. In any event, our results suggest that, throughout Late Pliocene and Pleistocene climate cycling, Southern Hemisphere atmosphere dynamics were tightly correlated and influential across a latitudinal range of at least 45°S to 80°S. We have also shown that a close concordance exists between this Southern Hemisphere atmospheric climate signal and the global ocean climate signal contained in oxygen isotope curves, at a resolution of ~1 to 2 ky and throughout much of the past 3.9 My. The reasons why most Southern Hemisphere climate records for MIS 1 to 5 differ so markedly at millennial scale from the proxy-climate signatures of Greenland and the North Atlantic remain elusive, but one possible explanation is that the North Atlantic signal is of regional significance only. Many previous discussions of the presumed "bipolar seesaw" have argued that the primary control on Northern and Southern Hemisphere differences is oceanographic rather than atmospheric (*19*). That the Site

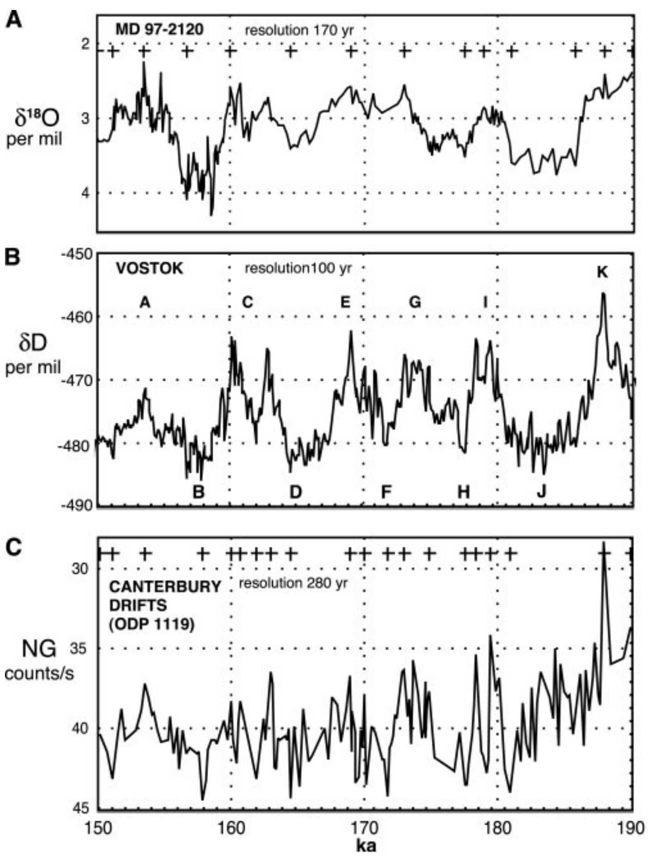

Fig. 3. Comparison between Southern Hemisphere marine and atmospheric climate records from MIS 6 (150 to 190 ky ago). (**A**) Planktic oxygen isotope curve for eastern New Zealand core MD97-2120 (*18*), a reoccupation of Site 594 (*17*). (**B**) Deuterium isotope ratio for the Vostok ice core (*15*), indicating interstadials 6A to 6K and stadials 6B to 6J. (**C**) Natural gamma-ray signal from ODP Site 1119 (reversed scale) (*13*).

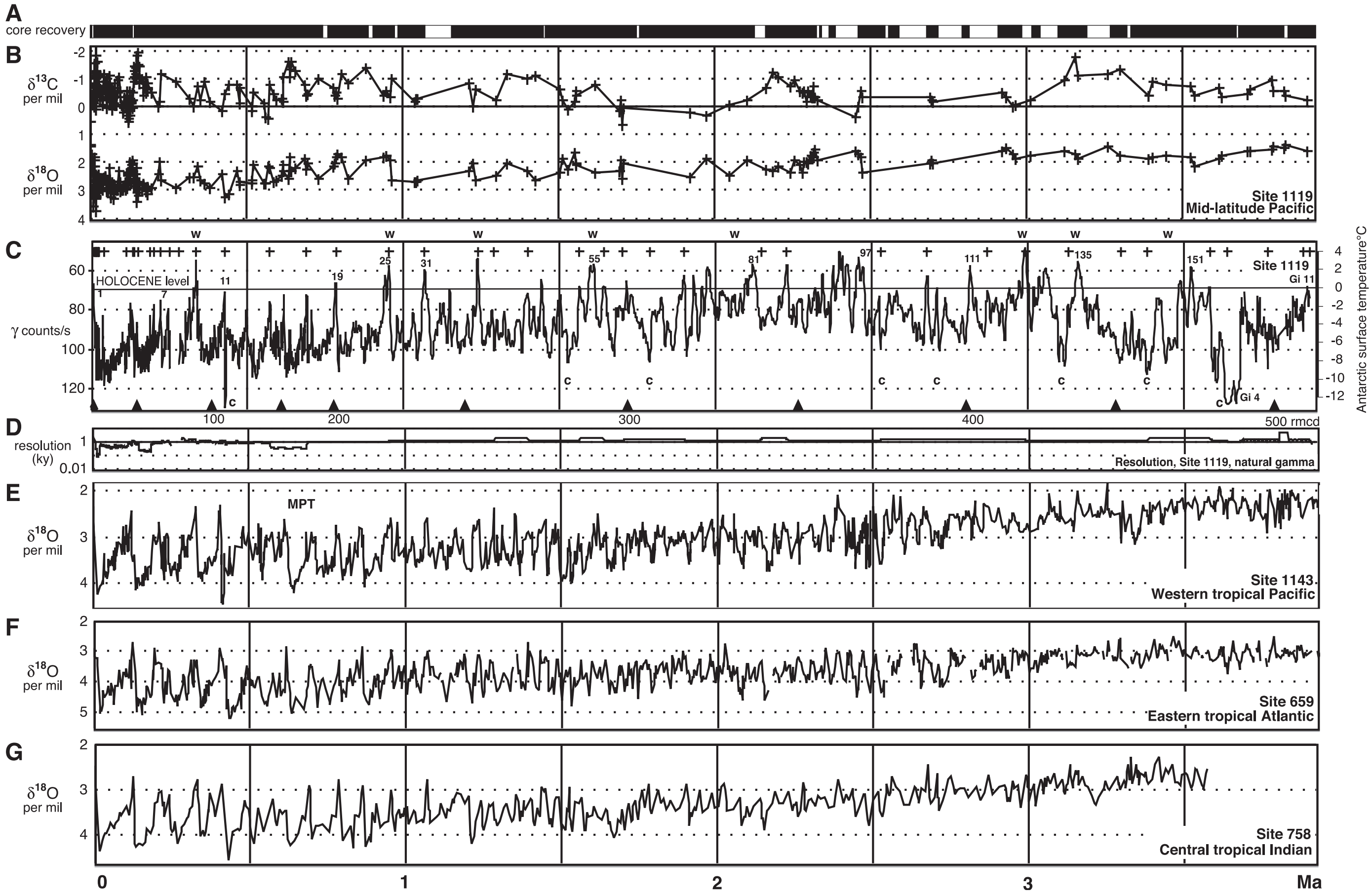

Fig. 4. Summary history of atmospheric and marine climatic cyclicity over the past 3.9 Ma. (**A**) Core retrieval from ODP Site 1119 (average recovery, 89%), which controls the completeness of the stable isotope record. (**B**) Carbon (upper) and oxygen (lower) isotopic measurements for Site 1119C. (**C**) Natural gamma ray record from ODP Site 1119 (reversed scale), produced by merging onboard MST measurements with downhole log measurements (*14*). The age scale is derived by matching climatic cycles at the points indicated by crosses to their MIS equivalents at Vostok and at ODP Sites 758 and 1143. Selected isotope stage equivalents are numbered; warm and cold climatic extrema are indicated by W and C above and below the gamma ray curve, respectively; basal triangles indicate incremental 50-m depths on the revised meters composite depth scale (*14*); and the right-hand scale indicates the possible Antarctic polar plateau air temperature equivalent for Site 1119 cyclicity, based on scaling the amplitude of the MIS 5 to 6 difference to the Vostok and Mt. Fuji deuterium records (*15*, *22*). (**D**) Sample resolution of gamma ray measurements for Site 1119 (logarithmic scale). MPT, Mid-Pleistocene Transition. (**E** to **G**) Benthic oxygen isotope records for the Pacific (Site 1143), Atlantic (Site 659), and Indian (Site 758) oceans, respectively (*14*).

1119 gamma record of atmospheric change and the MD97-2120, and perhaps ODP Site 983, oxygen isotope records match the Vostok record so closely at short time scales may suggest instead that climate change is primarily atmosphere-driven, through mechanisms such as changes in the North Atlantic Oscillation and the Pacific El Niño Southern Oscillation (*20*, *21*). Indeed, atmospheric rather than oceanic factors may have also controlled the multimillennial Dansgaard-Oeschger events of the North Atlantic region (*4*).

References and Notes

1. C. D. Charles, J. Lynch-Stiglitz, U. S. Ninnemann, R. G. Fairbanks, *Earth Planet. Sci. Lett.* **142**, 19 (1996).
2. L. Vidal *et al.*, *Clim. Dyn.* **15**, 909 (1999).
3. T. Blunier, E. J. Brook, *Science* **291**, 109 (2001).
4. C. Wunsch, *Quat. Sci. Rev.* **22**, 1631 (2003).
5. G. R. Clare, B. B. Fitzharris, T. J. H. Chinn, M. J. Salinger, *Int. J. Climatol.* **22**, 107 (2002).
6. J. Oerlemans, J. P. F. Fortuin, *Science* **258**, 115 (1992).
7. G. H. Denton, C. H. Hendy, *Science* **264**, 1434 (1994).
8. C. Singer, J. Shulmeister, B. McLea, *Science* **281**, 812 (1998).
9. R. M. Newnham, D. J. Lowe, *Geology* **28**, 759 (2000).
10. C. S. M. Turney, M. S. McGlone, J. M. Wilmshurst, *Geology* **31**, 223 (2003).
11. R. M. Carter, P. R. Gammon, L. Millwood, *Mar. Geol.* **205**, 29 (2004).
12. M. E. Raymo, in *Start of a Glacial*, G. J. Kukla, E. Went, Eds. (NATO Advanced Studies Institutes Series, Springer-Verlag, Berlin, 1992), vol. 13, p. 207.
13. R. M. Carter *et al.*, *Proc. ODP Init. Rep.* (Ocean Drilling Program, College Station, TX, 1999), **181**.
14. Materials and methods are available as supporting material on *Science* Online.
15. J. R. Petit *et al.*, *Nature* **399**, 429 (1999).
16. W. Dansgaard *et al.*, in *Late Cenozoic Glacial Ages*, K. K. Turekian, Ed. (Yale Univ. Press, New Haven, CT, 1971), p. 37.
17. C. S. Nelson, P. J. Cooke, C. H. Hendy, A. M. Cuthbertson, *Paleoceanography* **8**, 435 (1993).
18. K. Pahnke, R. Zahn, H. Elderfield, M. Schulz, *Science* **301**, 948 (2003).
19. W. S. Broecker, *Paleoceanography* **13**, 119 (1998).
20. R. D. S. Seager *et al.*, *Q. J. R. Meteorol. Soc.* **128**, 2563 (2002).
21. Although ocean-transferred signals do in general propagate more slowly than atmospheric signals, they can nevertheless move rapidly enough to preclude their resolution within millennial and possibly even centennial scale records. For instance, Haine *et al.* (*23*) have used chlorofluorocarbons as tracers to demonstrate that Antarctic Bottom Water from the Weddell Sea traveled more than 8500 km toward New Zealand in only 23 years.
22. O. Watanabe *et al.*, *Nature* **422**, 509 (2003).
23. T. Haine *et al.*, *J. Geophys. Res.* **103**, 27637 (1998).

24. We thank J. Tian, K. Pahnke, W. Prell, W. Howard, J. McManus, and D. Oppo for providing data used in the preparation of Figs. 2 to 4 and the accompanying discussion; R. Wust, L. Carter, and two referees for their constructive criticism of the manuscript; and the scientific, drilling and ship's staff of drilling Leg 181 and the staff of ODP–Texas A&M University for the hardworking contributions they made toward collecting, describing, archiving and sampling the core materials from Site 1119. This research used samples provided by the ODP, which is sponsored by NSF and participating countries under management of the Joint Oceanographic Institutions. Financial support was provided by the Australian Research Council (grant no. DP0344080) and by the University of Adelaide.

Supporting Online Material
www.sciencemag.org/cgi/content/full/304/5677/1659/DC1
Materials and Methods
SOM Text
Tables S1 to S3
References and Notes

17 November 2003; accepted 7 May 2004